Scientific paper

Stabilization of ZnS Nanoparticles in Micellar Dispersion of Cetyltrimethylammonium Bromide

Petr Praus,[1,*] Richard Dvorský,[2] Petr Kovář[3] and Jana Trojková[2]

[1] *Department of Analytical Chemistry and Material Testing, VŠB-Technical University of Ostrava, 17. listopadu 15, 708 33 Ostrava-Poruba, Czech Republic*

[2] *Institute of Physics, VŠB-Technical University of Ostrava, 17. listopadu 15, 708 33 Ostrava-Poruba, Czech Republic*

[3] *Department of Chemical Physics and Optics, Charles University in Prague, Faculty of Mathematics and Physics, Ke Karlovu 3, 121 16 Prague 2, Czech Republic*

** Corresponding author: E-mail: petr. praus@vsb.cz; Tel: +420 59 7321527*

Received: 16-02-2012

Abstract

ZnS nanoparticles were precipitated in micellar dispersions of cetyltrimethylammonium bromide (CTAB). ZnS nanoparticles and cetyltrimethylammonium (CTA^+) ions formed positively charged ZnS-CTA micelles with the mode zeta potential of 35 mV. The ZnS-CTA micelles were simulated by molecular modelling that confirmed the formation of positive CTA^+ bilayers on the ZnS surface. The large agglomerates of the ZnS-CTA micelles were observed by the dynamic light scattering (DLS) method and electron transmission microscopy (TEM). The size of the ZnS nanoparticles of about 5 nm was estimated from their band-gap energy obtained from UV spectra and electron transmission micrographs. The relationship between zeta potentials (ξ) and hydrodynamic sizes (d) was found as $\xi = 641/d - 5.9$.

Keywords: ZnS nanoparticles, Cetyltrimethylammonium bromide, Micellar dispersion, Molecular modelling

1. Introduction

Semiconductor nanoparticles such as metal oxides or metal sulphides are well known for their outstanding electrochemical properties, which make them utilizable for photooptics, optoelectronics, photocatalysis etc.[1] One of the most important factors related to nanomaterials is the dependence of physical and chemical properties on their size. The decrease of a semiconductor particle size leads to the increase of its specific surface area and band-gap energy, which is known as the quantum size effect or quantum confinement.[2,3] The large surface of nanoparticles results in their high catalytic activity. Oxidation and/or reduction reactions on semiconductor nanoparticles begin with the photoexcitation of electrons from a valence band to a conduction band generating positive holes, which further react with various organic and inorganic compounds.

Zinc sulphide is a semiconductor with a wide direct band gap energy of about 3.7 eV. ZnS nanoparticles have been synthesized by the precipitation of zinc ions with sulphide (solubility products $K_s = 1.6 \times 10^{-24}$ of sphalerite and 2.5×10^{-22} of wurtzite at 25 °C). Freshly prepared ZnS nanoparticles tend to agglomerate and, therefore, are mostly stabilized by macromolecules or surfactants. Cationic surfactants such as cetyltrimethylammonium,[4–8] sodium bis(2-ethylhexyl) sulphosuccinate,[9,10] L-cysteine and mercaptoethanol[11] and other stabilizers were used to prevent nanoparticles agglomeration. The stabilization of nanoparticles by their deposition on solid supports was also attempted. The SiO_2 matrix was covered by different amounts of ZnS, which led to its higher catalytic efficiency.[12] ZnS nanoparticles were also supported on laponite,[13] bentonite[14] and montmorillonite.[5,15]

Processes occurring on a nanoscale level cannot be observed by experimental methods but can be described and characterized by theoretical methods. One of suitable tools is molecular modelling based on empirical force fields. Total crystal energy of a system is consisted of bonded interactions describing the deformation of structure

and non-bonded interactions consisting of electrostatic and van der Waals energy contributions. Analysis of some energy characteristics can provide information on stability of systems, the mutual compatibility of their parts and estimation of a probability of some processes.

The aim of this work was to precipitate ZnS nanoparticles in the presence of micellar dispersions of CTAB. Unlike our earlier work,[15] in which the composite of ZnS nanoparticles and montmorillonite was prepared, here we tested a stabilizing role of CTAB with no solid support. Although interactions between CTAB and some nanoparticles were modelled by several authors[16,17] the interactions of ZnS nanoparticles and CTAB were firstly simulated in our previous paper.[18] Sublimation energies were calculated depending on the number and orientation of CTA^+ cations on the surface of ZnS nanoparticles. In this work, total crystal energy of a micelle composed from a ZnS core and dense CTA^+ cover was calculated. Existence of these micelles was confirmed by zeta potentials and hydrodynamic sizes measurements and by electron transmission microscopy.

2. Experimental

2. 1. Material and Chemicals

The used chemicals were of analytical reagent grade: zinc acetate, sodium sulphide (delete comma), (all from Lachema, Czech Republic), cetyltrimethyammonium bromide (Sigma chemical Co., USA). Water deionized by reverse osmosis (Aqua Osmotic, Czech Republic) was used for the preparation of all solutions.

2. 2. Precipitation of ZnS Nanoparticles

ZnS nanoparticles were precipitated by adding zinc acetate to sodium sulphide.[15] The precipitation was performed in the micellar dispersion of CTAB with the concentration of 3 mmol L^{-1}. The S^{2-}:Zn^{2+} ratio was kept at 1.5:1.

2. 3. Transmission Electron Microscopy

Transmission electron microscopy (TEM1) of the ZnS nanoparticles was performed with a JEM 2010 (Jeol, Japan) electron microscope at 160 kV of the acceleration voltage. For the TEM measurements, a drop of the aqueous dispersions of the ZnS nanoparticles and CTAB was deposited on the copper grids with a carbon layer.

Transmission electron microscopy (TEM2) was also performed on a JEM 1230 (Jeol, Japan) microscope operated at 80 kV. The freshly prepared samples of the ZnS nanoparticles stabilized by CTAB were placed on a copper grid (400 mesh) coated by a film of 1.5–3% of polyvinylformaldehyde in chloroform, dried by blotting paper and analyzed after 2 days. A contrast of micrographs was improved by 1% solution of ammonium molybdate added to the samples.

2. 4. UV-VIS Spectra Measurements

The UV-VIS absorption spectra of the ZnS-CTA colloidal dispersions were measured by a double-beam spectrometer Lambda 25 (Perkin Elmer, USA). All spectra were recorded using 1 cm quart cuvettes within the wavelength range of 200 nm to 800 nm.

2. 5. Zeta Potential and Dynamic Light Scattering Measurements

Zeta potential and dynamic light scattering measurements were performed using a Zetasizer Nano ZS instrument (Malvern Instruments, UK). A sample of the ZnS-CTA dispersion was filtered through a membrane filter with a pores size < 100 nm and injected into the disposable capillary cell (DTS1061). The measurements of the zeta potentials and hydrodynamic sizes d (nm) were performed up to 6 min after the precipitation using the SOP Player programme. In this manner, the fractions of nanoparticles with low zeta potentials could be registered before their flocculation.

2. 6. X-ray Powder Diffraction

The X-ray powder diffraction (XRD) study was performed by a powder diffractometer (BRUKER D8 ADVANCE) equipped with a scintillation and position-sensitive detector (VANTEC) and a source of CoKa radiation. The diffraction patterns were recorded in an ambient atmosphere under constant conditions (50 kV, 60 mA). The XRD patterns were identified using the PDF-2-Release 2004 database.

2. 7. Molecular Modelling

Molecular modelling simulations were carried out in the Forcite module of Materials Studio 4.3 modelling environment.[19] The wurtzite structure data were used for building the ZnS nanoparticles. Crystallographic data for wurtzite are the following: space group $P6_3mc$, $a = b =$ 0.382 nm, $c = 0.626$ nm.[20] According to experimental data nanoclusters in the shape of a sphere with the radii of 2.0 nm were created. The CTA^+ ion was built in the 3D sketcher module and its geometry was optimized in the Compass force field[21] in vacuum with partial charges assigned by the force field.

The CTA^+ ions were subsequently placed on the ZnS surface in a monolayer and bilayer arrangement (see Part 3.3). The length of CTA^+ measured between the nitrogen atom and the last carbon atom of the chain is about 2.1 nm. Taking into account the size of the ZnS particle, the distance between the ZnS surface and the closest carbon or nitrogen atom of CTA^+ depending on the CTA^+ arrangement the diameter of ZnS-CTA is about 10 nm. The CTA^+ ions oriented by their positive headgroups towards the outer

space were shifted with respect to those oriented in the opposite direction. The shift was from about 1/3 to 1/2 of the CTA^+ length. The models were optimized in the Universal force field22 and charges of the system were calculated by the Qeq method23. The molecular dynamics was carried out in the NVT statistical ensemble with a dynamics step of 0.5 fs and 400 ps of dynamics were performed.

3. Results and Discussion

3. 1. Preparation of ZnS Nanoparticles

The ZnS nanoparticles were precipitated in the presence of CTAB in the concentration of 3 mmol L^{-1} that was higher than its critical micellar concentration of about 1 mmol L^{-1} in water at 25 °C. This means that the ZnS nanoparticles coexisted with the CTAB monomers and micelles in their colloidal dispersions.

To determine size of the ZnS nanoparticles UV spectra of the ZnS-CTA dispersions were recorded. A typical absorption edge at about 318 nm is obvious in Figure 1.

The UV-VIS absorption spectra of nanoparticles are commonly used for the determination of band-gap energy (E_{bg}) according to the Tauc equation.[24] In this study we found the band-gap energy of 3.9 eV by means of the Tauc approach in the same manner as demonstrated in our previous study.[15] The band-gap energy was used for calculation of the ZnS nanoparticle radius by means of the Brus equation[3]

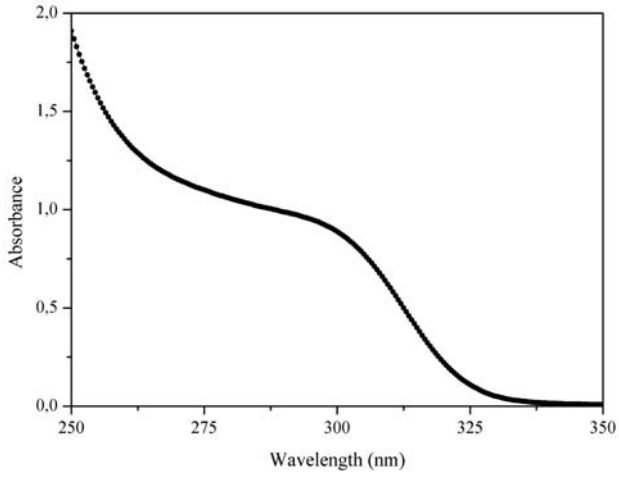

Figure 1. UV-VIS spectrum of ZnS-CTA dispersion.

$$E_{bg}(nano) = E_{bg}(bulk) + \frac{h^2}{8r^2}\left(\frac{1}{m_e} + \frac{1}{m_h}\right) - \left(\frac{1.8e^2}{4\pi\varepsilon_r\varepsilon_0 r}\right) \quad (1)$$

where $E_{bg}(nano)$ and $E_{bg}(bulk)$ are the band gap energies of bulk and nano ZnS, respectively, h is the Planck´s constant, r is the radius of the nanoparticle, m_e and m_h are the effective masses of electron and hole respectively and ε_r is the relative permittivity dielectric constant of the material, ε_o is the permittivity of vacuum. Here, $m_e = 0.42m_0$ and $m_h = 0.61m_0$, where m_0 is the free electron mass and ε_r = 8.76.[25] The radius was calculated at r = 2.1 nm.

3. 2. Electron Microscopy Study

The size of the ZnS nanoparticles was also determined from the TEM1 micrograph shown in Figure 2. One can see the nanoparticles were bound together by CTAB forming large agglomerates. The diameters of the ZnS nanoparticles were measured manually and their histogram is shown in the inset of Figure 2. The median diameter was 4.8 nm which agrees well with the calculated diameter $2r$ = 4.4 nm. The selected area electron diffraction revealed the wurtzite structure of the ZnS nanoparticles but the bulk ZnS particles precipitated without stabilization had the sphalerite structure determined by XRD. This structure change can be explained by the high pressure Δp inside the nanoparticles according to the Young-Laplace equation $\Delta p = 2\sigma/r$, where σ is the surface tension on particles.

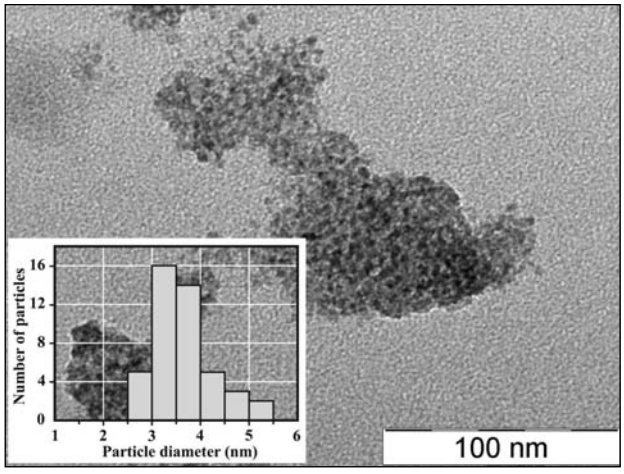

Figure 2. TEM1 micrograph of ZnS-CTA including size histogram.

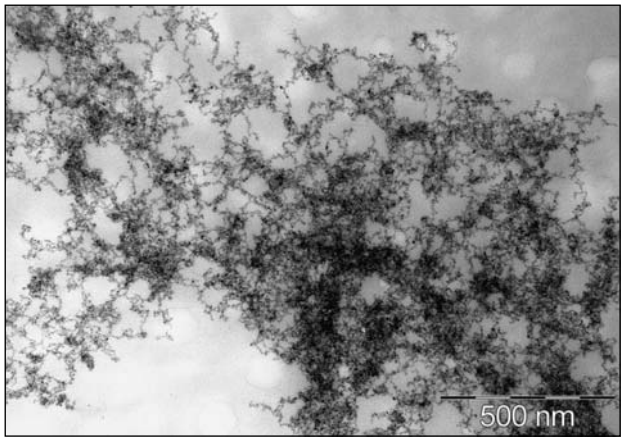

Figure 3 TEM2 micrograph of ZnS-CTA.

The TEM2 micrograph in Figure 3 demonstrates the morphology of the ZnS-CTA dispersions. As it is obvious the ZnS nanoparticles and CTAB were agglomerated into large flocs of various sizes also indicated by DLS (see below). Such a large floc is shown in Figure 2.

3. 3. ZnS-CTA Micelle Modelling

The original ZnS-CTA dispersions were characterized by the distribution functions of the zeta potentials and hydrodynamic sizes as demonstrated in Figure 4. From this figure it follows that, e.g. 84% of the nanoparticles had the zeta potentials higher than 30 mV. The mode (the number that appears most often in a set of numbers) of zeta potentials was 35 mV and the mode of hydrodynamic sizes was 16 nm. The positive zeta potentials indicated that the stable colloid dispersions of the positively charged ZnS-CTA micelles were formed.

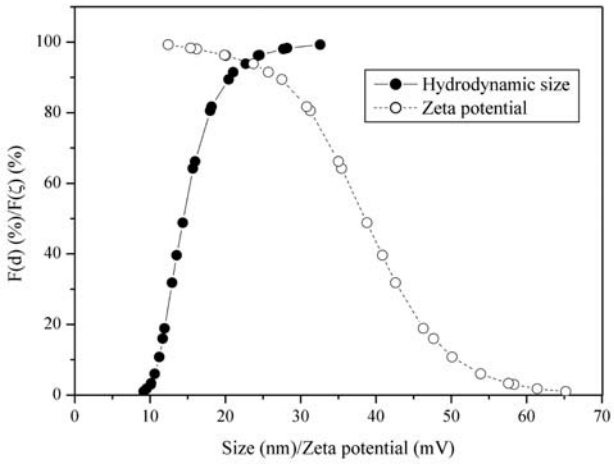

Figure 4. Distribution functions of zeta potentials F(ζ) and hydrodynamic sizes F(d) of ZnS-CTA micelles.

The relationship between the zeta potentials and the hydrodynamic sizes was calculated from their density functions as follows: $\xi = 641/d - 5.9$ ($r = 0.9976$). According to this equation the smaller particles had the higher zeta potentials as a result of the higher total surface area and the higher amount of adsorbed CTA^+ and *vice versa*.

Based on the measured positive zeta potentials, the ZnS nanoparticle and CTAB were supposed to create the ZnS-CTA micelle composed from the ZnS core and two adsorbed CTA^+ layers. The first CTA^+ layer was likely adsorbed directly with its headgroups to the ZnS surface, which is negatively charged as a result of adsorbed sulphides (the Paneth-Fajans rule). The second CTA^+ layer oriented by their positive headgroups from the nanoparticles should be bound to the first CTA^+ layers by means of hydrophobic interactions of their interlaced aliphatic chains. To confirm this idea the ZnS-CTA micelle was modelled by the molecular simulations.

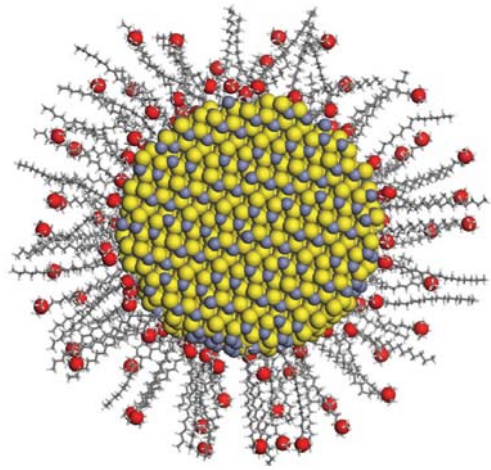

Figure 5. Midle cut of ZnS nanoparticle covered by CTA+ bilayer (R = 2.5 nm and N = 255). Positive headgroups are red, sulphur atoms are yellow and zinc atoms are gray.

Table 1. Calculated crystal energies for CTA^+ arrangements on ZnS nanoparticle

CTA^+ arrangement	Total energy (kJ mol^{-1})	Bonded energy (kJ mol^{-1})	Non-bonded energy (kJ mol^{-1})
Monolayer	–255277	144535	–399812
Bilayer	–328621	140796	–469417

The ZnS nanoparticle of wurtzite structure built from 1731 Zn^{2+} and S^{2-} ions was covered by 255 CTA^+ cations. In the first system, all 255 CTA^+ cations were arranged into a monolayer oriented with their polar headgroups towards the ZnS nanoparticle surface. In the second system, 255 CTA^+ cations were divided into the monolayer of 130 CTA^+ ones adsorbed to the ZnS nanoparticle and 125 CTA^+ ones oriented toward the aqueous dispersion (Fig. 5).

The stability of both systems was described by the total crystal energies. They are summarized in Table 1. In general, the total crystal energy is a sum of bonded and non-bonded crystal energies. Only models with the negative values of total energy can be considered as stable. The lower total energy values the higher stability of the model and the higher probability of the real structure based on this model. The total crystal energy of the bilayer arrangement was lower than that of the monolayer one, which indicates that the CTA^+ cations were arranged in two layers. It was ascribed mainly to the lower non-bonded energy contributions caused by a lower electrostatic repulsion between the polar headgroups in the double-layer arrangement. The distance between the polar headgroups and the hydrocarbon tails ranged from 0.6 nm to 1.3 nm.

4. Conclusion

The ZnS nanoparticles were precipitated in the micellar dispersions of CTAB forming the stable colloidal dispersions. The radius of ZnS nanoparticles of about 2.1 nm was calculated by the Brus equation and agreed well with r = 2.2 nm observed by TEM. The molecular simulations of the ZnS-CTA micelle confirmed that the CTA^+ bilayer was formed on the ZnS nanoparticle preferentially to the CTA^+ monolayer. The ZnS-CTA micelles and their agglomerates with the mode hydrodynamic diameter of 16 nm were positively charged as characterized by the mode zeta potential of 35 mV. The TEM micrographs showed the flocs of the ZnS-CTA micelles. The reciprocal relationship between the zeta potentials and the hydrodynamic sizes of the ZnS-CTA flocs was found. By our best knowledge this finding has not been described in the literature yet.

The nature of the ZnS-CTA micelles connection will be studied by molecular modelling in next research. The ZnS-CTA dispersions will be applied for the photocalytic reactions, e.g. photodecomposition of various organic compounds.

5. Acknowledgement

This work was supported by the Czech Science Foundation (P107/11/1918) and by the Regional Materials Science and Technology Centre (CZ.1.05/2.1.00/01.0040) in Ostrava.

6. References

1. D. Schroder, Semiconductor material and device characterization. John Wiley and Sons, New York, **2006**, pp. 780.
2. Z. Wang Z, N. Herron, *J. Phys. Chem*. **1991**, *95*, 525–532.
3. L. E. Brus, *J. Chem. Phys*. **1984**, *80*, 4403–4409.
4. A. Murugadoss, A. Chattopadhyay, *Bull. Mater. Sci*. **2008**, *31*, 533–539.
5. S. Miao, Z. Liu, B. Han, H. Yang, Z. Miao, Z. Sun, *J. Colloid Interf. Sci.* **2006**, *301*, 116–122.
6. S. K. Mehta, S. Kumar, S. Chaudhary, K. K. Bhasin, M. Gradzielski*, Nanoscale Res. Lett*. **2009**, *4*, 17–28.
7. S. K. Mehta, S. Kumar, M. Gradzielski, *J. Colloid Interf. Sci.* **2011**, *360,* 497–507.
8. M. K. Naskar, A. Patra, M. Chatterjee, *J. Colloid Interface Sci*. **2006**, *297*, 271–275.
9. J. Zhang, M. Xiao, Z. Liu, B. Han, T. Jiang, J. He, G. J. Yang, *J. Colloid Interf. Sci.* **2004**, *273*, 160–164.
10. P. Calandra, M. Goffredi, V. T. Liveri, *Colloids Surf. A*, **1999**, *160,* 9–13.
11. A. Chatterjee, A. Priyam, S. C. Bhattacharya, A. Saha, *Colloids Surf. A*, **2007**, *297*, 258–266.
12. P. Johne, H. J. Kisch *Photochem. Photobiol. A: Chem*., **1997**, *111*, 223–228.
13. J. Németh, I. Dékány, *Colloid. Polym. Sci.* **2000**, *278*, 211–219.
14. M. Ghiaci, M. E. Sedaghat, H. Aghaei, A. Gil, *J. Chem. Technol. Biotechnol.* **2009**, *84*, 1908–1915.
15. O. Kozák, P. Praus, K. Kočí, M. Klementová, *J. Colloid Interface Sci.* **2010,** 352, 244–251.
16. C. J. Yang, X. Chen, Z. M. Sui, L. Y. Wang, *Colloids Surface A.* **2006**, *274*, 219–222.
17. J. Yue, X. C. Jiang, Q. H. Zeng, A. B. Yu, *Solid State Sci.* **2011**, *12*, 1152–1159.
18. P. Praus, R. Dvorský, P. Horínková, M. Pospíšil, P. Kovář, *J. Colloid Interf. Sci*. **2012**, *377*, 58–63.
19. Materials Studio Modeling Environment, Release 4.3 Documentation. Accelrys Software Inc., San Diego, **2003**.
20. J. W. Anthony, R. A. Bideaux, K. W. Bladh, M. C. Nichols, (Eds.), Handbook of Mineralogy. Mineralogical Society of America, Chantilly, VA 20151–1110, USA.
21. H. Sun, D. Rigby, *Spectrochim. Acta A*, **1997**, *53*, 1301–1323.
22. A. K. Rappe, C. J. Casewit, K. S. Colwell, W. A. Goddard, W. M. Skiff, *J. Am. Chem. Soc.* **1992**, *114*, 10024–10035.
23. A. K. Rappe, W. A. Goddard, *J. Phys. Chem* **1991**, *95*, 3358–3363.
24. J. Tauc, Amorphous and Liquid Semiconductors. Plenum Press, New York, **1974**, pp. 441.
25. K. Dutta, S. Manna, S. K. De, *Synth. Met*. **2009**, *159*, 315–319.

Povzetek

ZnS nanodelce smo oborili v micelarnih disperzijah cetiltrimetilamonijevega bromida (CTAB). Nanodelci ZnSin cetiltrimetilamonijevi (CTA^+) ioniso tvorili pozitivno nabite micele ZnS-CTA z vrednostjo zeta potenciala 35 mV. S pomočjo molekularnega modeliranja smo potrdili nastanek pozitivno nabitih dvoplasti CTA^+na površini ZnS. Velike aglomerate micel ZnS-CTA smo opazovali z metodo dinamičnega sipanja svetlobe (DLS) in elektronsko mikroskopijo. Velikost nanodelcev je bila na osnovi vrednosti energije prepovedanega pasu in posnetkov presevnega elektronskega mikroskopa ocenjena na 5 nm. Zveza med zeta potencialom (ξ) in hidrodinamično velikostjo delcev (d) je $\xi = 641/d - 5{,}9$.